

Master's Thesis♣

Petrology of Saprolites in Central Hesse

Oluwatobiloba Odukoya

December 17, 2024

Submitted to the University of Freiburg
Geology - Institute of Mineralogy and Petrology
Faculty of Environment and Natural Resources

universität freiburg

University of Freiburg
Geology - Institute of Mineralogy and Petrology
Faculty of Environment and Natural Resources

Author	Oluwatobiloba Odukoya, Matriculation Number: 5364725
Editing Time	June 20, 2024 - December 17, 2024
Examiners	Dr. Lukas Gegg, Department of Sedimentary Geology and Quaternary Research Department of Geology
Supervisor	Prof. David Dolejs, Institute of Mineralogy and Petrology Department of Geology
Declaration	<p>I hereby declare, that I am the sole author and composer of this Thesis and that no other sources or learning aids, other than those listed, have been used. Furthermore, a full list of works used to develop this work, to which I cannot claim ownership, has been referenced.</p> <p>I also declare, that my Thesis has not been prepared for another examination or assignment, either wholly or excerpts thereof.</p> <p>Lastly, I declare that the electronic version of the submitted master thesis corresponds in content and format to the copies printed on paper.</p>

Place, Date

Signature

Abstract

The comprehensive analysis of saprolites from various lithologies endemic to Central Hesse has provided valuable insights into the weathering processes and products of Tertiary Europe. Through the integration of petrology, micromorphology, grain size analysis, and geochemistry, a detailed picture of formation conditions has emerged. Geochemical analyses reveal a consistent enrichment of immobile elements and depletion of alkali components, highlighting the intensity of chemical weathering. Secondary mineralizations of hematite, goethite, and siderite further confirm the transformative effects of weathering on the original rock compositions. Petrographic observations complement these findings, showcasing fine-grained textures, clay coatings, and flow structures indicative of fluid activity. Collectively, these features point to weathering as the dominant alteration mechanism, with little evidence of hydrothermal interference.

The observed alteration patterns provide valuable insights into past climatic conditions, suggesting a history of intense weathering regimes. These results have broader implications for reconstructing paleoenvironments and understanding the mobility of elements during weathering. Additionally, the study highlights the need for methodological advancements in grain size analysis, particularly for fine-grained materials, to improve measurement accuracy. By integrating multidisciplinary approaches, this research contributes to unraveling the complexities of weathering processes and their implications for geological and environmental sciences.

In conclusion, this study underscores the transformative impact of weathering on saprolites, driven by a combination of chemical, physical, and mineralogical processes. Past climatic conditions have facilitated intense chemical weathering, aided by fluid transport, resulting in highly altered mineral assemblages enriched in immobile elements, some of which hold economic significance. These findings enhance our understanding of weathering dynamics and provide a foundation for future investigations into the interplay between geology, climate, and surface processes.

Zusammenfassung

Die umfassende Analyse von Saproliten aus verschiedenen in Mittelhessen vorkommenden Lithologien hat wertvolle Einblicke in die Verwitterungsprozesse und -produkte des tertiären Europas geliefert. Durch die Integration von Petrologie, Mikromorphologie, Korngrößenanalyse und Geochemie ist ein detailliertes Bild der Bildungsbedingungen entstanden. Geochemische Analysen zeigen eine konsistente Anreicherung von immobilisierbaren Elementen und eine Verarmung von Alkalibestandteilen, was die Intensität der chemischen Verwitterung verdeutlicht. Sekundäre Mineralisierungen von Hämatit, Goethit und Siderit bestätigen die transformativen Auswirkungen der Verwitterung auf die ursprüngliche Gesteinszusammensetzung. Petrographische Beobachtungen ergänzen diese Ergebnisse und zeigen feinkörnige Texturen, Tonüberzüge und Fließstrukturen, die auf flüssige Aktivitäten hinweisen. Insgesamt deuten diese Merkmale auf Verwitterung als vorherrschenden Alterationsmechanismus hin, wobei es kaum Anzeichen für hydrothermale Störungen gibt.

Die beobachteten Alterationsmuster bieten wertvolle Einblicke in die klimatischen Bedingungen der Vergangenheit und lassen auf eine Geschichte intensiver Verwitterungsregime schließen. Diese Ergebnisse haben weitreichende Auswirkungen auf die Rekonstruktion von Paläoumgebungen und das Verständnis der Mobilität von Elementen während der Verwitterung. Darüber hinaus unterstreicht die Studie den Bedarf an methodischen Fortschritten bei der Korngrößenanalyse, insbesondere bei feinkörnigem Material, um die Messgenauigkeit zu verbessern. Durch die Integration multidisziplinärer Ansätze trägt diese Studie dazu bei, die Komplexität von Verwitterungsprozessen und ihre Auswirkungen auf die Geologie und die Umweltwissenschaften zu entschlüsseln.

Zusammenfassend unterstreicht diese Studie die transformativen Auswirkungen der Verwitterung auf Saprolite, die durch eine Kombination von chemischen, physikalischen und mineralogischen Prozessen angetrieben werden. Die klimatis-

chen Bedingungen der Vergangenheit haben eine intensive chemische Verwitterung begünstigt, die durch den Flüssigkeitstransport unterstützt wurde und zu einer stark veränderten Mineralzusammensetzung führte, die mit immobilen Elementen angereichert ist, von denen einige wirtschaftliche Bedeutung haben. Diese Ergebnisse verbessern unser Verständnis der Verwitterungsdynamik und bieten eine Grundlage für künftige Untersuchungen des Zusammenspiels zwischen Geologie, Klima und Oberflächenprozessen.

Acknowledgments

I am deeply grateful to my supervisor, Prof Dolejs, for his invaluable guidance, support, and encouragement throughout this research. His expertise and dedication have been instrumental in shaping the direction and success of this work.

To my classmates, especially Nico Nöthen and Edwin Wambicho, I appreciate your camaraderie and insightful discussions, which made this journey both intellectually stimulating and enjoyable. To the wonderful staff at the department that lent me their wisdom, expertise and precious time.

On a personal note, I owe a heartfelt thanks to my family for their unwavering support, patience, and encouragement. Your belief in me has been my greatest source of strength.

Finally, I dedicate this work to Alethea Harrison, my muse and my inspiration.

Contents

Figure Index	VIII
--------------	------

Table Index	XII
-------------	-----

1	Introduction	1
1.1	Problem Statement	3
1.2	Chemical Weathering and Soil Formation	3
1.3	Analytical Methods for Grain Size Determination	8
1.3.1	Principles of Laser Diffraction Analysis	9
1.3.2	Principles of Köhn Pipette Analysis	10
1.4	Thesis Objective	10
2	Geological Setting	12
2.1	Taunus	14
2.2	Westerwald	16
2.3	Vogelsberg	17
3	Analytical Methods	20
3.1	Petrography	22
3.1.1	Macrophotography	22
3.1.2	Microphotography	22
3.2	Grain Size Distribution	23
3.2.1	Wet Sieving Method	24
3.2.2	Laser Diffraction Analysis	25
3.2.3	Köhn-Pipette Analysis	27
3.3	Whole-Rock Geochemical Analysis	28
3.3.1	ICP-OES and ICP-MS	29
3.3.2	IR Spectrometry	30
3.3.3	Titration	31

4	Results	32
4.1	Geography of Samples	32
4.2	Petrography and Micromorphology	35
4.2.1	Macroscopic Description	35
4.2.2	Observations from Microphotographs	42
4.3	Grain Size Analysis	47
4.3.1	Köhn Method (Using Sedimat 4-12)	47
4.3.2	Laser Diffraction (Using Mastersizer 3000)	52
4.4	Geochemical Analysis	56
4.4.1	Whole Rock Geochemistry	56
4.4.2	Chemical Parameters and Weathering Indices	58
4.4.3	Normative Composition	58
4.4.4	Classification and Discrimination Diagrams	60
5	Discussion	67
5.1	Comparison of Grain Size Determinations: Mechanical vs. Diffraction Methods	68
5.2	Interpretation of Weathering Processes	71
6	Conclusion	72
6.1	Future Work	73
	References	1

Figure Index

1.1	Anotated Diagram of the Saprolite Layer Juxtaposing Pedological and Geological Division of the Profile	5
2.1	Showing study area dimensions (maps.google.com)	12
2.2	Sample locations relative to their position on a map of Hesse . . .	13
2.3	Regional Geology of Study Area Modified from (BGR, 2018) . . .	14

2.4	Showing the Taunus and its Division into subunits (De-academic.com, 2024)	16
2.5	Shows the Westerwald with its Tertiary deposits and Volcanic extent (Roček & Wuttke, 2010)	17
2.6	Showing distribution of volcanics of the Vogelsberg Volcanic field (Bogaard & Wörner, 2003)	19
3.1	Flow Chart of Analytical Procedures	20
3.2	Flow Diagram for measurement with FTIR Spectroscopy Tribonet (2024)	30
4.1	Geological map of study area showing sample location and the geology that underlay them (modified from BGR (2018)	34
4.2	Field observations of basalt samples: A) BE1, BE2 & BE3; B) BE4; C) BE5; D) BL1; E) BL2 & BL3	36
4.3	Basalt samples: A) BE1; B) BE2; C) BE3; D) BE4; E) BE5; F) BL1; G) BL2; H) BL3; I) BW	37
4.4	Field observations of carbonate samples: A) CB; B) CH1, CH2 & CH3	38
4.5	Carbonate samples: A) CB; B) CF; C) CH1; D) CH2; E) CH3; F) CH4	39
4.6	Field observations of slate samples: A) SB; B) SE3; C) SE1 & SE2; D) SL & SL2	40
4.7	Slate samples: A) SB; B) SE1; C) SE2; D) SE3; E) SH; F) SL; G) SL2; H) SW	41
4.8	Microphotographs of basalt samples: A) BE1; B) BE2; C) BE3; D) BE4; E) BE5; F) BL2; G) BL3; H) BW	43
4.9	Microphotographs of carbonate samples: A) CB/1; B) CB/2; C) CF/1; D) CF/2; E) CH1; F) CH2; G) CH3; H) CH4	45
4.10	Microphotographs of slate samples: A) SE3; B) SL2/1; C) SL2/2; D) SW	46
4.11	Cumulative Frequency Distribution Plot for Basalt Samples from Sedimat 4-12 Data	47
4.12	Cumulative Frequency Distribution Plot for Carbonate Samples from Sedimat 4-12 Data	50
4.13	Cumulative Frequency Distribution Plot for Slate Samples from Sedimat 4-12 Data	51

4.14	Grain Size Distribution Plot for Basalt Saprolites from Mastersizer Data	52
4.15	Grain Size Distribution Plot for Carbonate Saprolites from Mastersizer Data	53
4.16	Grain Size Distribution Plot for Slate Saprolites from Mastersizer Data	55
4.17	Quartz-Alkali-Plagioclase-Feldspathoid Classification Diagram from CIPW-norm data (Streckeisen, 1976) (BE1=1, BE2=8, BE3=17, BE4=11, BL1=7, BL2=0, BL3=10, CB=15, CH1=19, CH2=2, SB=18, SE1=12, SE2=6, SE3=5, SH=4, SL=3, SW=9)	60
4.18	Albite-Anorthite-Orthoclase Classification (O'Connor 1965) (BE1=1, BE2=8, BE3=17, BE4=11, BL1=7, BL2=0, BL3=10, CB=15, CH1=19, CH2=2, SB=18, SE1=12, SE2=6, SE3=5, SH=4, SL=3, SW=9)	61
4.19	Al ₂ O ₃ -CaO-FeO/MgO Discrimination Diagram	62
4.20	Al ₂ O ₃ -CaONa ₂ O-K ₂ O Discrimination Diagram	62
4.21	Classification diagram of Herron (1988) for Discriminating Sediment Types	63
4.22	Discrimination Diagram of Ross and Bedard (2009) for Discriminating Mafic Rocks	64
4.23	Incompatible Elements Spider Plot for NMORB by Pearce (2014) (BE1=1, BE2=8, BE3=17, BE4=11, BL1=7, BL2=0, BL3=10)	65
4.24	Incompatible Elements Spider Plot for Sediments by Plank (2014) (BE1=1, BE2=8, BE3=17, BE4=11, BL1=7, BL2=0, BL3=10, CB=15, CH1=19, CH2=2, SB=18, SE1=12, SE2=6, SE3=5, SH=4, SL=3, SW=9)	65
4.25	REE Chondrite Spider Plot by Anders & Grevesse (1989) (BE1=1, BE2=8, BE3=17, BE4=11, BL1=7, BL2=0, BL3=10, CB=15, CH1=19, CH2=2, SB=18, SE1=12, SE2=6, SE3=5, SH=4, SL=3, SW=9)	66
5.1	Comparison of Grain Size Distribution Results from Sedimat 4-12 and Mastersizer 3000 for Basalts	69
5.2	Comparison of Grain Size Distribution Results from Sedimat 4-12 and Mastersizer 3000 for Carbonates	70

5.3	Comparison of Grain Size Distribution Results from Sedimat 4-12 and Mastersizer 3000 for Slates	70
-----	--	----

Table Index

3.1	Table 3.1: The Schedule of Analytical Methods	21
3.2	Grain Size Analysis Methods Overview	24
3.3	Standard Operating Procedures (SOPs) for Mastersizer 3000 . . .	26
4.1	Sample locations and coordinates	33
4.2	Results from Analysis with Sedimat 4-12 on Carbonate and Basalt Saprolites	48
4.3	Results from Analysis with Sedimat 4-12 on Slate Saprolites . . .	49
4.4	Results from Analysis with Mastersizer 3000 on Basalts Saprolites	52
4.5	Results from Analysis with Mastersizer 3000 on Carbonate Saprolites	53
4.6	Results from Analysis with Mastersizer 3000 on Slates Saprolites .	54
4.7	Whole-Rock Geochemistry Results	57
4.8	Key Geochemical Parameters	58
4.9	CIPW normative composition according to O'Connor (1965) . . .	59

Chapter 1

Introduction

Saprolites, which are also known as “Weathering mantles” or “Grus” (especially concerning weathering granites), are a widespread feature of landscapes on every continent, occurring at or near the earth’s surface. They are most prominent in tropical to subtropical regions where they regularly exceed depths of 50 m Stoops, Marcelino, and Mees (2018), however, saprolites are not restricted to these locations as they can be as small as a few millimetres thick in temperate regions. In Europe, the distribution of saprolites is varied but is of significant quantities as they are present in central, western, and northern Europe. Locations where the presence of saprolites is well documented include the Iberian Peninsula, the Massif Central in France, parts of the Rhenish Massif in Germany (our study area), the British Isles, the Scandinavian Mountains, and the Fennoscandian Shield Migoñ and Lidmar-Bergström (2001); Vazquez (1981).

The word “Saprolite” was coined from the Greek for “rotten rock” (*/saproslithos/*) by G.F. Becker (1895) to describe bedrock still in the process of pedogenesis and delineate it from the layers further down the line of decomposition. They are the weathering remains of preexisting rocks exposed to atmospheric conditions such as precipitation, diurnal temperature changes, microbial activity, and high oxygen fugacity. They are the product of mineral transformations driven by thermodynamics, as the formation conditions at depth significantly differ from the conditions they encounter after their host rocks are exhumed. Saprolites differ from other weathering products because they remain in situ, meaning they develop as a covering, lying directly on top of the unweathered rock, like an outer skin. Due to this lack of mobilization, they also retain their rock fabric, even though the degree to which the fabric preservation varies with depth. The exact rate of weathering and thickness of the weathering mantle depends on the time spent at or close to the surface, the climate, and the rock type Ehlen (2005).

Saprolites frequently constitute a part of a more extensive stratigraphic sequence and usually only serve as a subordinate layer within the weathered profile. The weathered profile or regolith, as a whole, is an aggregate of layers of rock pieces in various stages of disintegration and originating from multiple sources. The A-B-C scheme was first introduced by Orth (1873, 1875) and later evolved by Dokuchaev, Vasily (1879a, 1879b). Improvements by Fowler (1925) brought the scheme to what is recognized today as the most widely accepted approach to the description of soil profiles Tandarich, Darmody, Follmer, and Johnson (2002). However, even though there is a unification of the scheme, there is no unification of the terms within the scheme, and the components are modified by authors to represent a variety of features studied, as evidenced by the review of Tandarich Tandarich et al. (2002).

The German soil classification scheme, as defined in the KA5 Eckelmann et al. (2006), begins the weathered profile with a layer littered with organic material that has just begun to humify and is known as the “O Horizon.” Below this layer is a completely disaggregated and unstructured layer which has lost all structure due to some varying combinations of biological and environmental processes and is known as the “A Horizon” or topsoil. The next layer, called the “E Horizon,” is where acids formed during humification of the organic matter in the previous layers, strip elements from the minerals in its layer and precipitates them further down, in a process called podzolization. Next is the “B Horizon,” which is structurally similar to the A Horizon but includes precipitates formed from the leaching processes in the layers above and less organic material. After that is the “C Horizon,” which has begun to weather but still preserves the structure of the bedrock below it. This layer corresponds to the titular saprolites and can be characterized as being the closest in density to the unaltered bedrock and the least affected by soil-forming processes of all the horizons.

Saprolites are studied by geochemists, civil engineers, hydrologists, geomorphologists, soil scientists, and exploration geoscientists for different purposes. They can serve as aquifers from which groundwater can be tapped or may form hosts for economic deposits through secondary or supergene enrichment for resources such as gypsum, clays, aluminium, manganese, nickel, copper, uranium, iron, gold, and other heavy minerals. Saprolites also serve as a window to the past, through which the events that led to their formation can be observed. Therefore, their study is important to understanding and predicting the effects of current geo-climatic processes.

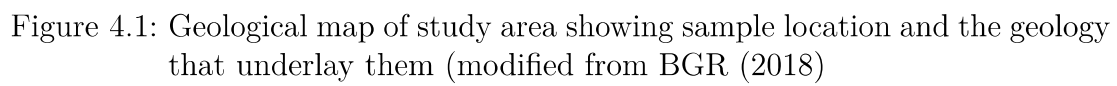
Chapter 2

Geological Setting

The study was carried out in localities in and around Central Hesse. The localities range from Weickartshain in eastern Giessen (central Hesse) to Liebenseid in southern Siegen (North-Rhine Westphalia) and Wasenbach in north-eastern Rhein-Lahn-Kreis (Rhineland Palatinate). A general triangulation of the area is shown in Figure 2.1 and shows that the samples come from an area encompassing a total of 1,432 km².



Figure 2.1: Showing study area dimensions (maps.google.com)



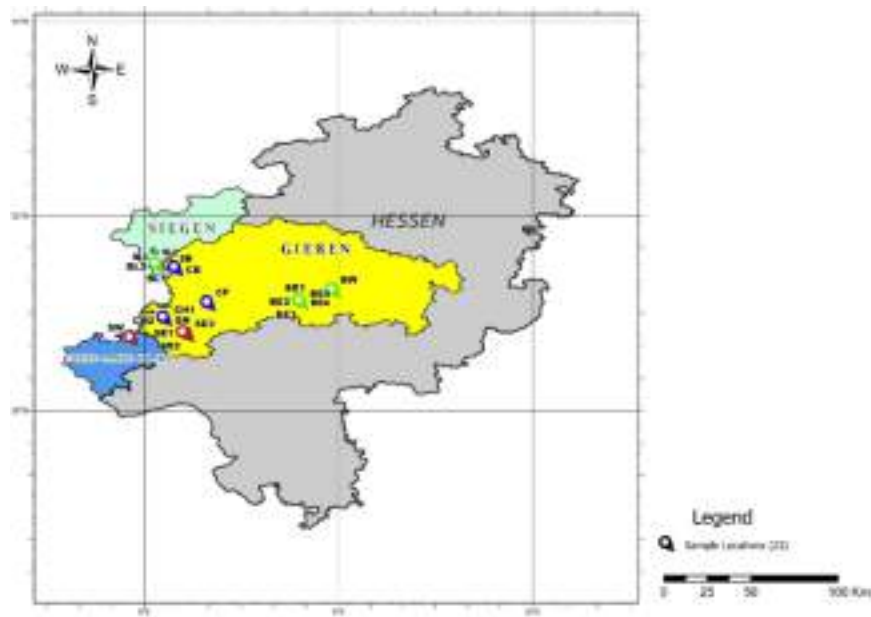


Figure 2.2: Sample locations relative to their position on a map of Hesse

The regional geology of the study area varies greatly in formation time and lithology. The area is chiefly underlain by metasedimentary rocks from the late Palaeozoic era that are crosscut in various locations by Cenozoic volcanics. There are also various sedimentary units stretching geochronologically between the Palaeozoic and the Cenozoic. The units belong to geological provinces of the Rhenish Massif or Rhenish Slate Mountains (“Rheinisches Schiefergebirge” in German) and the Hessian Depression (“Hessische Senke” in German), both of which have been affected by the tectonics of the Tertiary period. The Rhenish massif is made up of smaller geological units and the units which were sampled are the Taunus and Westerwald, located in the southern eastern portion of the province. The Hessian Depression also hosts a number of geological units and the unit of interest to our study is the Vogelsberg volcanic field. The three significant units are shown in Figure 2.3 and would be discussed individually for the rest of the chapter.

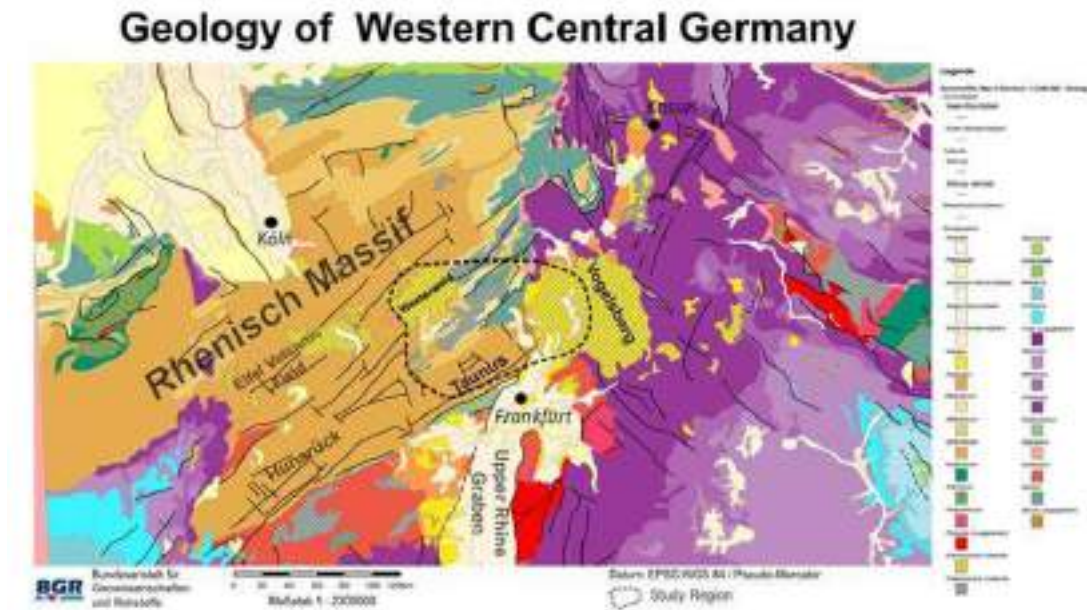


Figure 2.3: Regional Geology of Study Area Modified from (BGR, 2018)

2.1 Taunus

Taunus is the name given to a NW-SE striking mountain range located between Lorch am Rhein and Bad Nauheim with a length of about 75 km Toussaint (2024). It has a shared formation history with the adjacent Hunsrück hills, which are located on the other side of the Rhine river, as both resulted from orogenic events. The mountains are characterized by rugged ridges, deeply incised river valleys and broad plateaus. Together with the Hunsrück hills, they form the southern base of the Rhenish massif.

The Taunus as a geologic structural unit began as series of sedimentary facies that underwent tectonic compression between the Devonian and the Carboniferous periods Doublier, Potel, Franke, and Roache (2012). This was followed by episodic uplift from the Oligocene through to the Quaternary (low rates in the present day) and volcanism that formed two of the largest volcanics in Germany (Vogelsberg and Westerwald) from the Oligocene to the Quaternary El-Kelani, Jentzsch, and Schreiber (1998); Felix-Henningsen (2018); Haase, Goldschmidt, and Garbe-Schönberg (2004); Todt and Lippolt (1980). According to (Felix-Henningsen, 1994a, 2003, 2018) weathering began in the Rhenish massif in a tropical to sub-tropical paleoclimate during the Upper Mesozoic. This series of events resulted

Chapter 3

Analytical Methods

A total of twenty-three samples were selected to be investigated using the analytical methods discussed in this chapter. After the samples were collected from the field, they were air-dried in open plastic sampling bags between March 2024 and August 2024. A brief overview of the samples selected for each method is given in Figure 3.1. Following this is a detailed description of the procedures for each method.

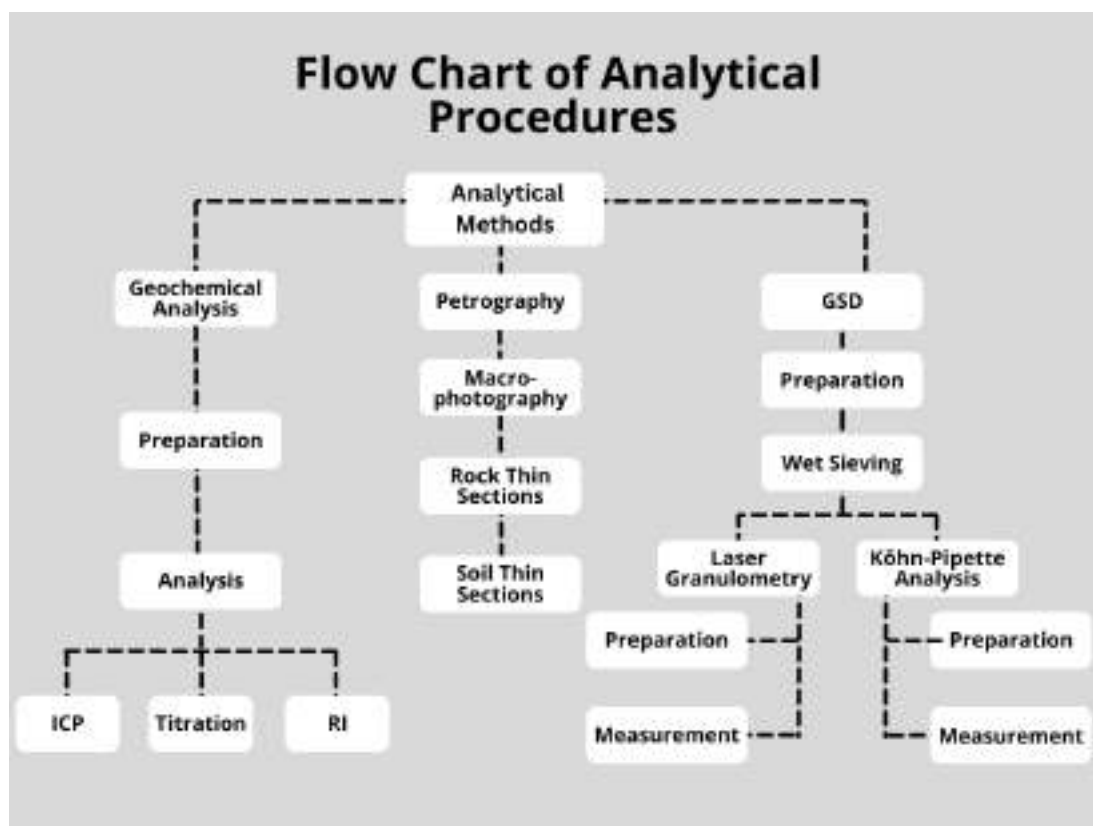


Figure 3.1: Flow Chart of Analytical Procedures

Table 3.1: Table 3.1: The Schedule of Analytical Methods

		Methods					
No.	Samples	WR-GCH	Microphotography		Macro-	Grain Size Distribution	
			Rock Sect	Soil sect	photog- raphy	Sedimat	Mastersizer
Slate saprolites							
1	SB	✓				✓	✓
2	SE1	✓			✓		
3	SE2	✓			✓	✓	✓
4	SE3	✓		✓	✓	✓	✓
5	SH	✓			✓	✓	✓
6	SL	✓				✓	✓
7	SL2		✓✓ ^a		✓		
8	SW	✓		✓	✓	✓	✓
Carbonate saprolites							
9	CB	✓	✓✓ ^a		✓		
10	CF		✓✓ ^a		✓		
11	CH1	✓		✓	✓	✓	✓
12	CH2	✓		✓	✓	✓	✓
13	CH3			✓	✓	✓	✓
14	CH4			✓	✓		
Basalt saprolites							
15	BE1	✓	✓		✓	✓	✓
16	BE2	✓	✓		✓	✓	✓
17	BE3	✓	✓		✓	✓	✓
18	BE4	✓	✓		✓		
19	BE5		✓		✓		
20	BL1	✓	✓		✓		
21	BL2	✓	✓		✓		
22	BL3	✓			✓		
23	BW			✓	✓		

^a a double tickmarks indicate that there are two samples for these lithologies

4.4.4 Classification and Discrimination Diagrams

The data above is presented in this final section as mineral classification and geotectonic classification plots to help classify the saprolites and also to observe how much they deviate from their ideal chemistry.

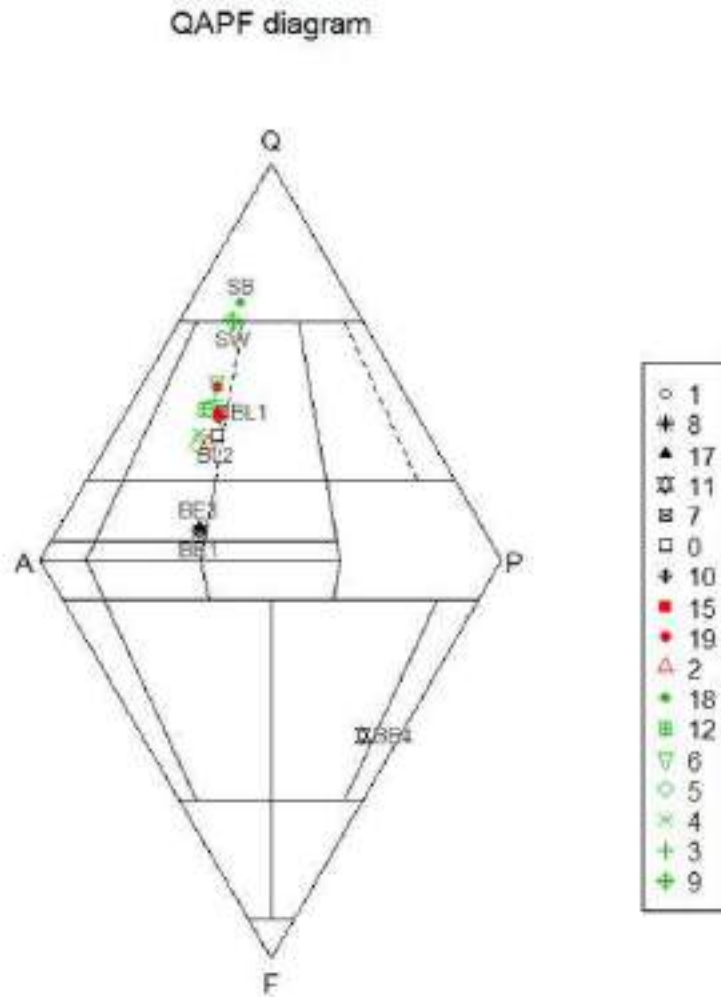


Figure 4.17: Quartz-Alkali-Plagioclase-Feldspathoid Classification Diagram from CIPW-norm data (Streckeisen, 1976) (BE1=1, BE2=8, BE3=17, BE4=11, BL1=7, BL2=0, BL3=10, CB=15, CH1=19, CH2=2, SB=18, SE1=12, SE2=6, SE3=5, SH=4, SL=3, SW=9)

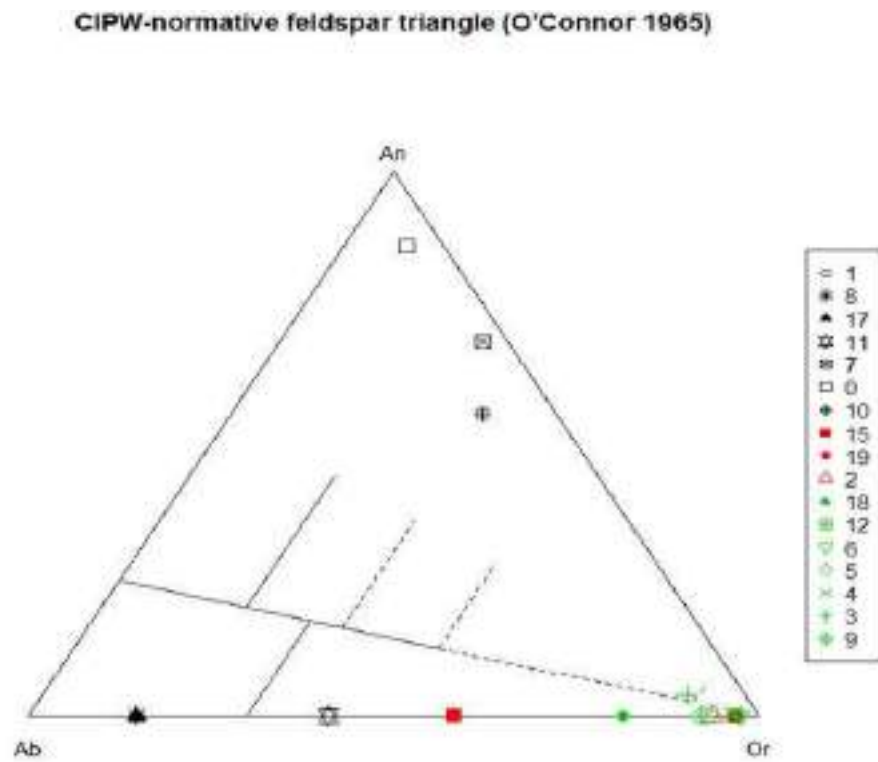
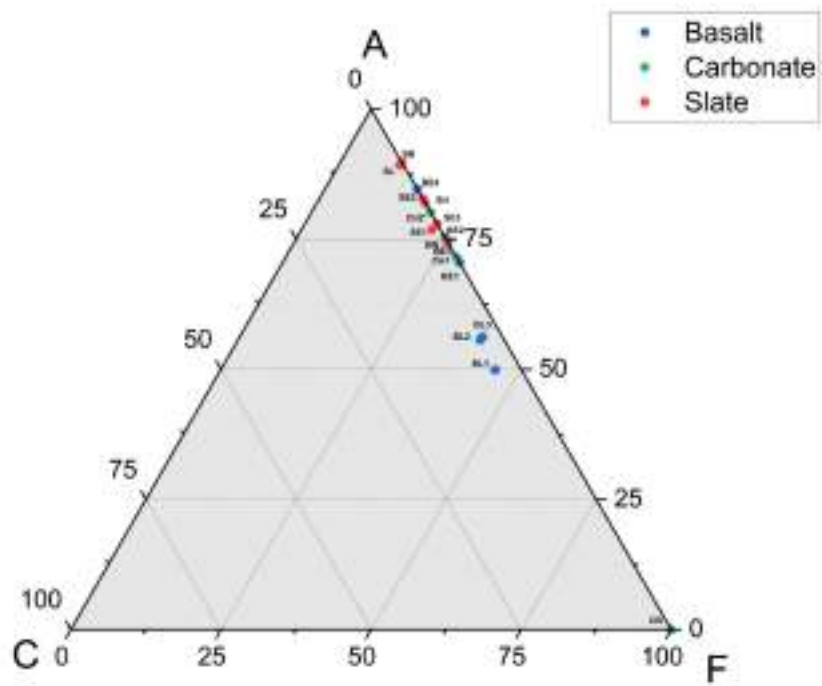
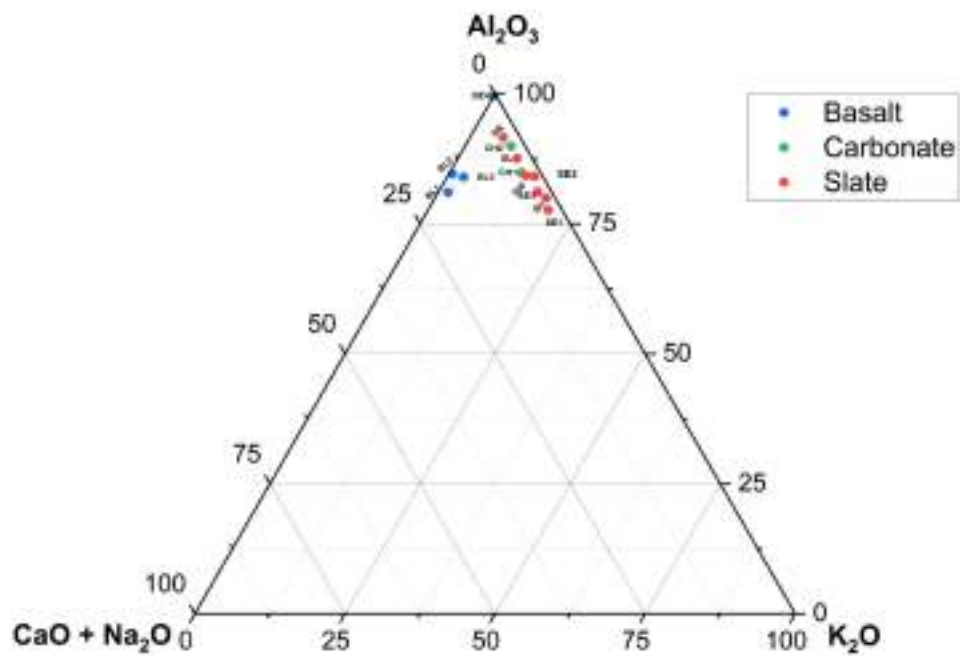


Figure 4.18: Albite-Anorthite-Orthoclase Classification (O'Connor 1965) (BE1=1, BE2=8, BE3=17, BE4=11, BL1=7, BL2=0, BL3=10, CB=15, CH1=19, CH2=2, SB=18, SE1=12, SE2=6, SE3=5, SH=4, SL=3, SW=9)

Figure 4.19: Al_2O_3 -CaO-FeO/MgO Discrimination DiagramFigure 4.20: Al_2O_3 -CaONa₂O-K₂O Discrimination Diagram

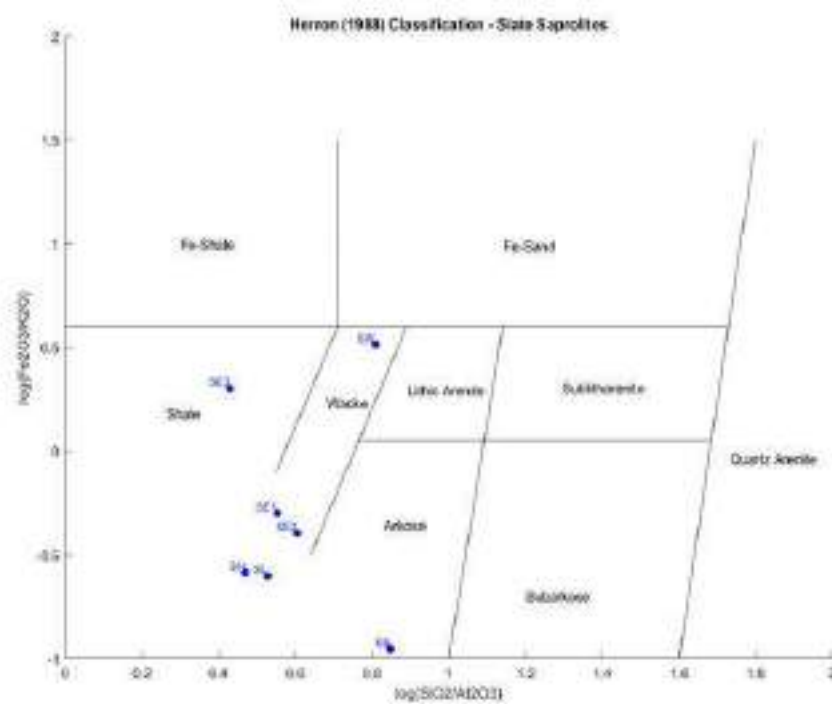


Figure 4.21: Classification diagram of Herron (1988) for Discriminating Sediment Types

Chapter 5

Discussion

Discussion This chapter discusses the results obtained from the analysis of the saprolites from three precursor rock types. The results are brought to life by comparing the findings with those from other studies in the region, as well as distant localities with similar settings. The results from the grain size determination are also examined, as the results of the two methods defer quantitatively.

The results in the previous chapter confirm the alteration of the samples from the various precursor rocks analysed. The premise for the study was established, as the extent of alteration observed is not commensurate with the current climatic conditions. The evidences that support the alteration to be by weathering are first discussed here. The weathering indices show that there is significant alteration in all saprolite precursors. From the petrography and geochemistry, it can be seen that all lithologies are significantly enriched in oxides of iron, titanium and aluminium. This increase was seen to coincide with a depletion in alkali oxides, which was especially observable in the carbonate samples which had unexpectedly low CaO values. The low CaO values were coupled with unexpectedly low CO₂ values which indicate that they had been hitherto lost. The basalt saprolites were also observed to have high LOI values of up to 25 % (wt). In Addition to all these, the petrography revealed an abundance of flow structures left behind by the action of fluids. These evidences however prove that the precursor rocks are altered but doesn't point us in the direction of weathering or hydrothermal alteration.

To differentiate between these two types of alterations, we first look at the mineral assemblages. Petrographically, the secondary mineral products of hematite, goethite and siderite along with the opaque oxides in the groundmass and clay coatings on crystals suggest the mineralization was achieved at temperatures closer to surface temperature. There are also no assemblages that indicate

hydrothermal, such as the absence of barite and fluorite that usually occurs with the formation of siderite in carbonate (Xie et al., 2023). Geochemically, the high concentration of Al oxides over the alkali oxides suggests that there was significant leaching of the alkali components or enrichment of Al oxides, both of which are only possibilities in places with intensive weathering regimes. Qualitatively, the two methods for grain size analysis confirm the abundance of fine-grained particles which have also been petrographically observed. While the formation of fine grains is not unique to the weathering process, it is sufficient to suggest that the adjacent kaolinite zones observed in the field could be genetically linked to the rocks sampled and profiles can be analysed in the future to trace the movement of the mobile elements.

In the Hunsrück area, which is about 30 km west of the general study area, the same weathering phenomena have been observed (Felix-Henningsen, 1994b; Felix-Henningsen & Spies, 1986; Sauer & Felix-Henningsen, 2006). Geochemical studies in the Ardennes Massif of Luxembourg by Moragues-Quiroga et al. (2017), are comparable to the results of our slate saprolites. The SiO₂ and Al₂O₃ values fit with that of the slates in our study, but when comparing the alkali component, our slates appear to be significantly depleted. Conversely, the iron content is higher in the slates from our study area, which signifies that the measured samples were more weathered than that chosen in the study of Moragues-Quiroga et al. (2017).

5.1 Comparison of Grain Size Determinations: Mechanical vs. Diffraction Methods

Grain size distribution is an important parameter of lithologies as they are one of the building blocks for the physical properties used for their identification. The study of the size distribution is typically most emphasized for sedimentary lithologies and thus, the methods have been optimized for this type of lithologies, especially quartzofeldspathic lithologies which are richer in coarser grains due to the resistance of quartz and feldspar to abrasion. This emphasis has resulted in the lack of innovation in the methods for the measurement of fine-grained materials which are usually of alternate mineralogy.

In this study, the Koehn method and the laser diffraction method have both been applied to ensure the accuracy of the results. However, while they are equally qualitative, they did not produce quantitative results that matched one

another. Results from both methods have been recast to cumulative frequencies and are presented in Figures 5.1 to 5.3. In the plots for the basalt and carbonate saprolites (Figures 5.1 and 5.2), a clear partition is seen between the two datasets belonging to the two methods. There is also a difference in the shapes of the curve profiles, which is significant because the gradient of the curves depict the rate of change of grain sizes which is a function of grain size sorting. The slate saprolites do not appear to have the same gap between the data sets and therefore the two sets of data roughly have the same shapes overall. The datasets for each method still differ by up to 20 % for the same data points, causing the significant underestimation or overestimation of significant classes necessary for the classification of the grain size distribution.

The problem is seen to arise due to the deviation from sphericity of clay minerals. Both methods make their measurements with the assumption that the particles being measured are spherical. In addition to this assumption of sphericity, the laser diffraction method also assumes a uniform density of materials being measured. Increasing abundances of clay minerals in samples propagates measurement uncertainty and increases errors in both methods.

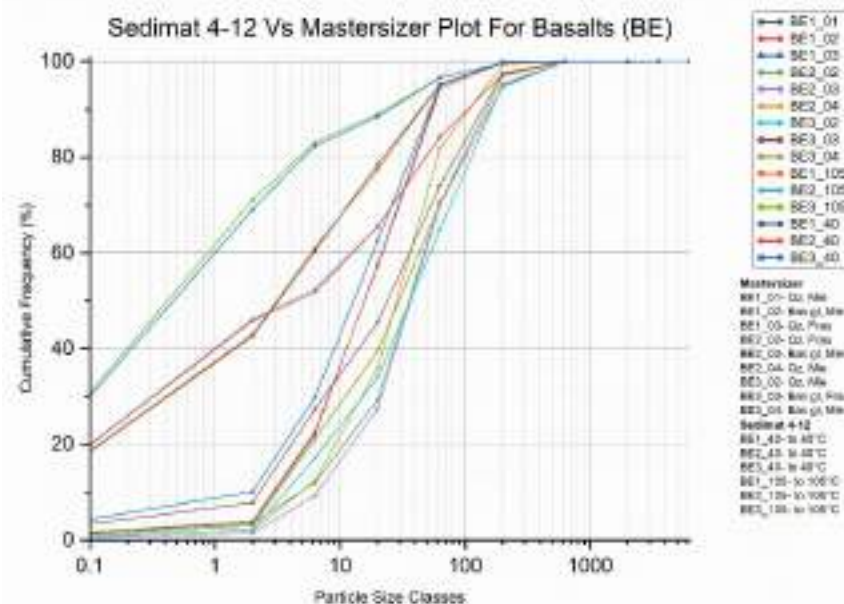


Figure 5.1: Comparison of Grain Size Distribution Results from Sedimat 4-12 and Mastersizer 3000 for Basalts

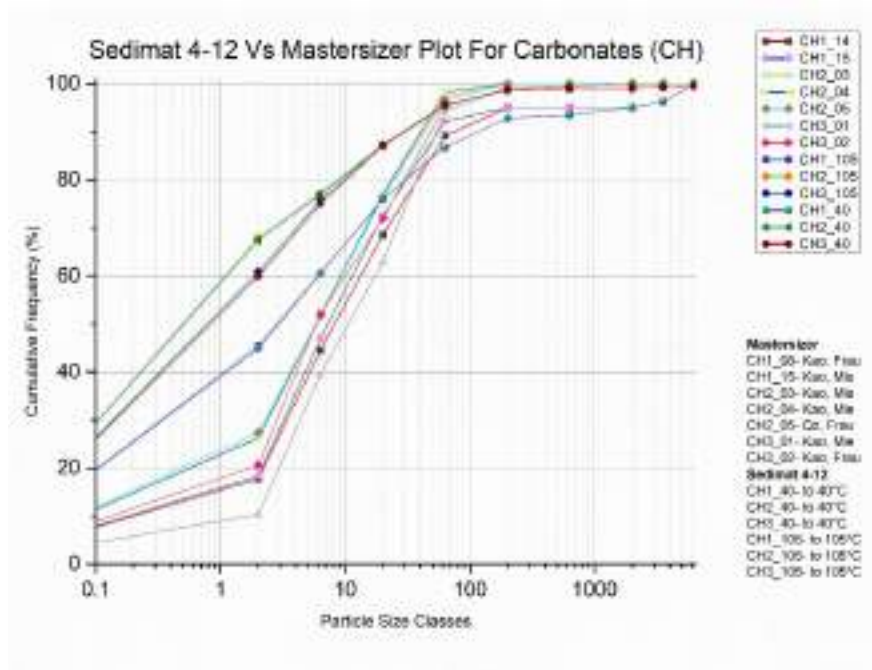


Figure 5.2: Comparison of Grain Size Distribution Results from Sedimat 4-12 and Mastersizer 3000 for Carbonates

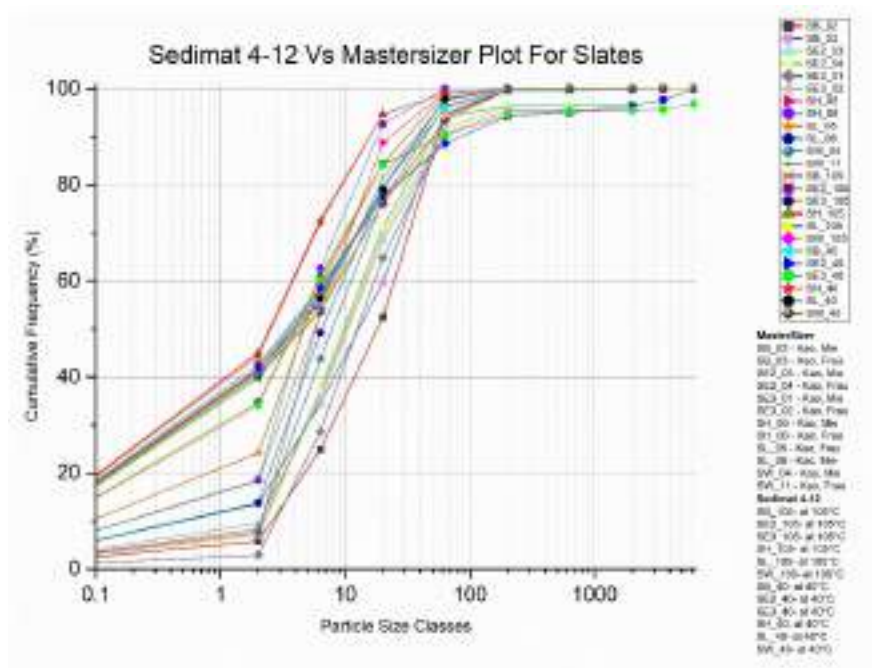


Figure 5.3: Comparison of Grain Size Distribution Results from Sedimat 4-12 and Mastersizer 3000 for Slates

5.2 Interpretation of Weathering Processes

The weathering process in these saprolites can be summarized as a system exhibiting high chemical activity, significantly enhanced by water as a transporting medium.. Chemical weathering leads to the breakdown of primary minerals, leaching of mobile elements, and formation of secondary minerals. This is evidenced by the geochemical trends and the petrographic observations of mineral replacements. This seems to have been consistently followed by redistribution by fluids, presumably exposing fresh surfaces for chemical weathering to re-intensify. This can be seen especially in the carbonate and slate samples with their relict water pathways.

Weathering intensity varies across samples, with some retaining more of their original characteristics (BE2 and BE5) while others show advanced alteration (BE3, BE4 and BL3). This variability likely reflects differences in local environmental conditions, exposure time, and inherent rock properties. The formation of secondary minerals, such as clays and iron oxides, plays a crucial role in the weathering process. These minerals not only contribute to the observed color changes but also influence the physical properties of the saprolite, such as porosity and permeability.

In conclusion, past climatic conditions has led to a suite of rocks that underwent intense chemical weathering aided by fluid transport. This has led to the formation of assemblages that are mineralogically highly altered to the state of enrichment in immobile elements which are economically significant in some cases.

References

- Becker, G. F. (1895). *Reconnaissance of the gold fields of the southern Appalachians*. US Government Printing Office.
- BGR, B. f. G. u. R. (2018). *GÜK250: Geological Map of Germany 1:250,000*. [\url{https://www.bgr.bund.de/}](https://www.bgr.bund.de/).
- Bogaard, P. J., & Wörner, G. (2003). Petrogenesis of Basanitic to Tholeiitic volcanic rocks from the Miocene Vogelsberg, Central Germany. *Journal of Petrology*, 44(3), 569–602. doi: 10.1093/petrology/44.3.569
- Bufe, A., Hovius, N., Emberson, R., Rugenstein, J. K. C., Galy, A., Hassenruck-Gudipati, H. J., & Chang, J.-M. (2021, apr). Co-variation of silicate, carbonate and sulfide weathering drives CO₂ release with erosion. *Nature Geoscience*, 14(4), 211–216. Retrieved from <https://www.nature.com/articles/s41561-021-00714-3> doi: 10.1038/s41561-021-00714-3
- Butt, C. R., Lintern, M. J., & Anand, R. R. (2000). Evolution of regoliths and landscapes in deeply weathered terrain - implications for geochemical exploration. *Ore Geology Reviews*, 16(3-4), 167–183. doi: 10.1016/S0169-1368(99)00029-3
- Chodorowski, J. (2011). Ortstein, Physical Properties. *Encyclopedia of Earth Sciences Series, Part 4*, 535. Retrieved from https://link.springer.com/referenceworkentry/10.1007/978-90-481-3585-1_252 doi: 10.1007/978-90-481-3585-1_252
- De-academic.com. (2024). *Vortaunus*. [\url{https://de-academic.com/dic.nsf/dewiki/1475701}](https://de-academic.com/dic.nsf/dewiki/1475701).
- Dokuchaev, Vasily, V. (1879a). *Cartography of Russian soils-Explanatory manual to the soil map of European Russia, as published by Division of Agriculture and Agroindustry (In Russian)* (Tech. Rep.). Saint Petersburg, Russia: Ministry of National Property. St.-Petersburg.
- Dokuchaev, Vasily, V. (1879b). *A short historical overview on the existing important soil classifications and critical examinations thereof. (In Russian)* (Tech. Rep.). Saint Petersburg, Russia: Bull. St.-Petersburg Society of

- Nature-Researchers.
- Doublier, M. P., Potel, S., Franke, W., & Roache, T. (2012). Very low-grade metamorphism of Rheno-Hercynian allochthons (Variscides, Germany): Facts and tectonic consequences. *International Journal of Earth Sciences*, 101(5), 1229–1252. doi: 10.1007/s00531-011-0718-3
- Eckelmann, W., Sponagel, H., Grottenthaler, W., Hartmann, K. J., Hartwich, R., Janetzko, P., ... Traidl, R. (2006). *Bodenkundliche Kartieranleitung. KA5*. Schweizerbart Science Publishers, Stuttgart, Germany.
- Eggerton, R. (2001). *The Regolith Glossary*.
- Ehlen, J. (2005). Above the weathering front: Contrasting approaches to the study and classification of weathered mantle. *Geomorphology*, 67(1-2 SPEC. ISS.), 7–21. doi: 10.1016/j.geomorph.2004.09.026
- El-Kelani, R., Jentzsch, G., & Schreiber, U. (1998). Gravity anomalies and subsurface geology in the Westerwald volcanic area, Germany. *International Journal of Earth Sciences*, 87(3), 381–393.
- Felix-Henningsen, P. (1994a). Mesozoic-Tertiary weathering and soil formation on slates of the Rhenish Massif, Germany. *Catena*, 21(2-3), 229–242. doi: 10.1016/0341-8162(94)90014-0
- Felix-Henningsen, P. (1994b). Mesozoic-Tertiary weathering and soil formation on slates of the Rhenish Massif, Germany. *CATENA*, 21(2-3), 229–242. Retrieved from <https://linkinghub.elsevier.com/retrieve/pii/0341816294900140> doi: 10.1016/0341-8162(94)90014-0
- Felix-Henningsen, P. (2003). THE MESOZOIC-TERTIARY WEATHERING MANTLE OF THE RHENISH MASSIF. In *Géologie de la France*. (pp. 71–75). Bureau de recherches géologiques et minières, Orléans.
- Felix-Henningsen, P. (2018, aug). Field Trip D (27 September 2018): characteristics and development of the Mesozoic-Tertiary weathering mantle and Pleistocene periglacial slope deposits in the Hintertaunus mountainous region. *DEUQUA Special Publications*, 1, 53–77. Retrieved from <https://deuquasp.copernicus.org/articles/1/53/2018/> doi: 10.5194/deuquasp-1-53-2018
- Felix-Henningsen, P., & Spies, E.-D. (1986). Soil development from Tertiary to Holocene and hydrothermal decomposition of rocks in the eastern Hunsrück area. *Mitteilungen der Deutschen Bodenkundlichen Gesellschaft*, 76–99.
- Fowler, E. D. (1925). Profile characteristics of some coastal plain soils. *Soil Science Society of America Journal*, 6(1), 19–23.

- Haase, K. M., Goldschmidt, B., & Garbe-Schönberg, C. D. (2004). Petrogenesis of tertiary continental intra-plate lavas from the Westerwald region, Germany. *Journal of Petrology*, 45(5), 883–905. doi: 10.1093/petrology/egg115
- Königshof, P., Becker, R. T., & Hartenfels, S. (2016). The Rhenish Massif as a part of the European Variscides. *Münstersche Forsch Geol Palaeontol*, 108, 1–13.
- Lippolt, H. J. (1983). Distribution of Volcanic Activity in Space and Time. In K. Fuchs, K. von Gehlen, H. Mälzer, H. Murawski, & A. Semmel (Eds.), *Plateau uplift* (pp. 112–120). Berlin, Heidelberg: Springer Berlin Heidelberg.
- Martha, S. O., Zulauf, G., Dörr, W., Nesbor, H.-D., Petschick, R., Prinz-Grimm, P., & Gerdes, A. (2014). The Saxothuringian-Rhenohercynian boundary underneath the Vogelsberg volcanic field: evidence from basement xenoliths and U-Pb zircon data of trachyte. *Zeitschrift der Deutschen Gesellschaft für Geowissenschaften*, 165(3), 373–394. doi: 10.1127/1860-1804/2014/0079
- Migoń, P., & Lidmar-Bergström, K. (2001). Weathering mantles and their significance for geomorphological evolution of Central and Northern Europe since the Mesozoic. *Earth-Science Reviews*, 56(1-4), 285–324. doi: 10.1016/S0012-8252(01)00068-X
- Moragues-Quiroga, C., Juilleret, J., Gourdol, L., Pelt, E., Perrone, T., Aubert, A., ... Hissler, C. (2017). Genesis and evolution of regoliths: Evidence from trace and major elements and Sr-Nd-Pb-U isotopes. *CATENA*, 149, 185–198. doi: 10.1016/j.catena.2016.09.015
- Nesbitt, H. W., & Young, G. M. (1982). Early Proterozoic climates and plate motions inferred from major element chemistry of lutites. *Natur*, 299(5885), 715–717. Retrieved from <https://ui.adsabs.harvard.edu/abs/1982Natur.299..715N/abstract> doi: 10.1038/299715A0
- O'Connor, J. T. (1965). A classification for quartz-rich igneous rocks based on feldspar ratios. - *U S Geological Survey, 525B, Professional Papers undefined 1965*. Retrieved from <https://cir.nii.ac.jp/crid/1574231874664577792>
- Orth, A. (1873). Das geologische Bodenprofil nach seiner Bedeutung für den Bodenwerth und die Landeskultur. *Nach d. Club d. Landw. Berlin*.
- Orth, A. (1875). *Die geognostisch-agronomische Kartirung mit besonderer Berücksichtigung der geologischen Verhältnisse Norddeutschlands und der Mark Brandenburg: erläutert an der Aufnahme vom Rittergut Friedrichsfelde bei Berlin; vom Landwirthschaftlichen Centralverein de* (Vol. 1). Verlag von

- Ernst & Korn.
- Parker, A. (1970). An Index of Weathering for Silicate Rocks. *Geological Magazine*, 107(6), 501–504. Retrieved from <https://www.cambridge.org/core/journals/geological-magazine/article/abs/an-index-of-weathering-for-silicate-rocks/7B19B352C8321E523E11A125361E9CA9> doi: 10.1017/S0016756800058581
- Roček, Z., & Wuttke, M. (2010, dec). Amphibia of Enspel (Late Oligocene, Germany). *Palaeobiodiversity and Palaeoenvironments*, 90(4), 321–340. Retrieved from <http://link.springer.com/10.1007/s12549-010-0042-0> doi: 10.1007/s12549-010-0042-0
- Salamon, M., & Königshof, P. (2010). Middle Devonian olistostromes in the Rheno-Hercynian zone (Rheinisches Schiefergebirge) - An indication of back arc rifting on the southern shelf of Laurussia. *Gondwana Research*, 17(2-3), 281–291. Retrieved from <http://dx.doi.org/10.1016/j.gr.2009.10.004> doi: 10.1016/j.gr.2009.10.004
- Sauer, D., & Felix-Henningsen, P. (2006). Saprolite, soils, and sediments in the Rhenish Massif as records of climate and landscape history. *Quaternary International*, 156-157(SPEC. ISS.), 4–12. doi: 10.1016/j.quaint.2006.05.001
- Schmitt, L. (2024). *Genetic processes of Lahn-Dill-type iron ores: insights from mineralogy, geochemistry and isotopes*. Dissertation, Bochum, Ruhr-Universität Bochum, 2024.
- Schreiber, U. (1996). Tertiärer Vulkanismus des Westerwaldes. *Terra Nostra - Exkursionsführer* 148, 187–212.
- Schwarz, T. (1997). Lateritic bauxite in central Germany and implications for Miocene palaeoclimate. *Palaeogeography, Palaeoclimatology, Palaeoecology*, 129(1-2), 37–50. doi: 10.1016/S0031-0182(96)00065-X
- Stoops, G., Marcelino, V., & Mees, F. (2018). *Interpretation of Micromorphological Features of Soils and Regoliths*. doi: 10.1016/C2009-0-18081-9
- Tandarich, J. P., Darmody, R. G., Follmer, L. R., & Johnson, D. L. (2002). Historical Development of Soil and Weathering Profile Concepts from Europe to the United States of America. *Soil Science Society of America Journal*, 66(2), 335–346. doi: 10.2136/sssaj2002.3350
- Todt, W., & Lippolt, H. J. (1980). K-Ar age determinations on Tertiary volcanic rocks: V. Siebengebirge, Siebengebirge- Graben. *Journal of Geophysics - Zeitschrift für Geophysik*, 48(1), 18–27.

- Tonui, E., Eggleton, T., & Taylor, G. (2003). Micromorphology and chemical weathering of a K-rich trachyandesite and an associated sedimentary cover (Parkes, SE Australia). *CATENA*, 53(2), 181–207. doi: 10.1016/S0341-8162(02)00200-X
- Toussaint, B. (2024). *Geologie des Taunus*. Retrieved from <http://www.taunuswelten.de/das-gebirge/geologie-des-taunus/>
- Tribonet. (2024). *Fourier Transform Infrared Spectroscopy*. \url{https://www.tribonet.org/wiki/fourier-transform-infrared-spectroscopy/}.
- Vazquez, F. M. (1981). Formation of gibbsite in soils and saprolites of temperate-humid zones. *Clay Minerals*, 16(1), 43–52. Retrieved from <https://www.cambridge.org/core/journals/clay-minerals/article/abs/formation-of-gibbsite-in-soils-and-saprolites-of-temperatehumid-zones/E3B676AAA5B3E48BEEA8A32DB2BA91A9> doi: 10.1180/CLAYMIN.1981.016.1.03
- Volker, F., & Menges, S. (2018). Field Trip A (23 September 2018): geology and geomorphology of Giessen and its surrounding areas. *DEUQUA Special Publications*, 1, 3–13. doi: 10.5194/deuquasp-1-3-2018
- Wedepohl, K. H. (1985). Origin of the Tertiary basaltic volcanism in the northern Hessian Depression. *Contributions to Mineralogy and Petrology*, 89(2-3), 122–143. Retrieved from <https://link.springer.com/article/10.1007/BF00379448> doi: 10.1007/BF00379448/METRICS
- Xie, M., Ma, F., Chen, G., Zheng, X., Xiao, R., & Zhang, C. (2023). Genesis and Geological Significance of Siderite in the First Member of the Nantun Formation of Dongming Sag, Hailar Basin. *Minerals 2023*, Vol. 13, Page 804, 13(6), 804. Retrieved from <https://www.mdpi.com/2075-163X/13/6/804/htmhttps://www.mdpi.com/2075-163X/13/6/804> doi: 10.3390/MIN13060804
- Ziegler, P. A. (1992). European Cenozoic rift system. *Tectonophysics*, 208(1-3), 91–111. doi: 10.1016/0040-1951(92)90338-7
-